Segmental Mobility in Deformed Amorphous Polymeric Networks. 1. Theory

B. Erman† and L. Monnerie*

Laboratoire de Physicochimie Structurale et Macromoléculaire, associé au C.N.R.S., E.S.P.C.I., 10 rue Vauquelin, 75231 Paris Cedex 05, France. *Received April 30, 1986*

ABSTRACT: A general theory of the relationship of orientational dynamics of chain segments to the state of deformation, swelling, and temperature is given. The molecular model of a real network with local constraints on junction fluctuations is adopted. Segmental mobility is expressed as a function of the molecular deformation tensor and the tensor denoting deformation of the domains in which chain sequences are embedded. The dynamics is assumed to be affected by configurational changes in chains upon stretching and by changes in the strength of coupling of sequences to their environments. Anisotropy of motion, i.e., differences in the mobility of sequences along different directions in the network, is assumed to be proportional to the segmental orientation function. Calculations based on the real network model exhibit features in mobility that cannot be predicted by the use of the classical affine or phantom network models. The validity of the assumptions of the theory and of calculations based on them is supported by experimental evidence presented in the following paper.

Introduction

In a bulk amorphous polymer far above the glass transition temperature, segments of chains possess a high degree of orientational mobility. The origin of segmental dynamics in the bulk, like that for the single chain, resides within transitions of sequences of units from one isomeric state to the other. Recent experimental investigations using the fluorescence anisotropy decay technique have shown that the segmental orientation autocorrelation function in the melt far above the glass transition temperature has the same form as that observed for dilute and concentrated solutions[1-4] with different correlation times.

Segmental mobility in a polymer chain results from correlated motions of several consecutive bonds, both in the dilute solution and in the bulk state. It has further been shown by fluorescence anisotropy decay studies that in bulk polybutadiene, for example, the motions occurring in the nanosecond range at 100 °C above the glass transition temperature involve coordinated motions of about six monomer units.[5] Correlated rearrangements of these units in the bulk are readily seen to be susceptible to the effects of steric constraints from the local environment. As a consequence of such steric constraints, the characteristic relaxation times of segmental orientations in the bulk are strongly affected by temperature and dilution with a suitable solvent.[6]

The segmental dynamics resulting from transitions among isomeric states is identical in a melt of long chains and in an undisturbed network in which the cross-link density is sufficiently low so that the glass transition temperature of the polymeric material is not affected. This follows from the fact that the immediate environment of a segment in both is the same and that the extent of entanglement of a chain to its environment in the undisturbed state is essentially proportional to the number of chains in contact with it.

The situation in the deformed network is different, however, from that in the unperturbed melt. Upon deformation, two mechanisms come into action. First, the dimensions of chains transform in accordance with the macroscopic strain, leading to a selective orientation of bond sequences along a chain with respect to the chain end-to-end vector and to a redistribution of isomeric states of the chains. The elastic action of entanglements imposes further local strains on portions of the chains, resulting in additional rearrangement of rotational states of sequences embedded in the entanglement domains. That such conformational changes are within the experimentally measurable range has been shown for polystyrene[7] stretched above the glass transition temperature. Recent experiments on deformed polyisoprene networks have shown that the extent of conformational rearrangements is also significant in this system.[8]

The second mechanism is due to the effect of local intermolecular interactions on the mobility of sequences along a chain. The extent of steric hindrances depends on the state of strain. The strength of constraints affecting a given sequence diminishes along directions of extension and increases along directions of compression.[9] The net effect averaged over all directions at a point may result in a decrease or increase of constraints, depending on the nature of the macroscopic strain and the structure of the network. Both of these mechanisms directly affect the mobility of segments. The extent of the first effect, i.e., of isomerization of bond sequences upon deformation, has been emphasized by various theoretical molecular models[10,11] describing local polymer dynamics. These models predict that the mobility of a given chain sequence is strongly controlled by its conformational state. In the following, we refer to this effect on mobility as the *conformational effect*. The latter mechanism described in the preceding paragraphs, i.e., the change of the strength of entanglements by strain, is the *steric effect*. A sequence of segments in a chain, embedded in the domain of constraint, is under the action of the environment through local intermolecular correlations. A detailed discussion of the mechanisms involved in this coupling was presented recently in relation to local segmental orientation in deformed networks.[12]

The conformational effect results from the intramolecular statistics of chains, whereas the steric effect originates from local intermolecular correlations. Both operate independently but simultaneously in a deformed network.

The purpose of the present study is to relate orientational mobility to the state of strain, swelling, temperature, and network structure. In the first section below, the relationship of deformation at the molecular level to the macroscopic state of strain is reviewed. Previous work on segmental orientation[12,13] and strain birefringence[14,15] has indicated that the use of the macroscopic strain tensor to represent transformations of average molecular dimensions is not satisfactory and that a more detailed discussion of deformation at the molecular level is required. In subsequent sections, mean orientational mobility and anisotropy

† Permanent address: School of Engineering, Bogazici University, Bebek, Istanbul, Turkey.

0024-9297/86/2219-2745$01.50/0

of mobility in a deformed network are formulated and related to the state of microscopic deformation.

The theory is developed according to the molecular model of real networks introduced some years ago by Flory.[9] According to this model, the space-filling properties of real chains are the sources of entanglements that operate in a deformed network. The theory has subsequently been shown to successfully describe various phenomena in networks.[16]

Recent advances in spectroscopic techniques allow for accurate measurement of the mobility of vectors affixed to chains.[6] Measurements can be performed directly on the native chain by employing the ^{13}C NMR or transient Kerr effect techniques. Measurements may also be performed by labeling certain sequences along the chains as in the ^{2}H NMR technique. Fluorescence polarization and electron spin resonance relaxation techniques, where labeling with molecules different from the chain backbone are required, may also be used for accurate representation of mobility in networks. The theory developed in this paper is general, in the sense that it may be used to describe results of the wide range of experiments mentioned. Predictions of the present theory are compared with results of fluorescence polarization experiments on polyisoprene networks in the following paper.[17]

Microscopic State of Strain in a Deformed Network

The geometry of local deformation in a network and its dependence on macroscopic strain are reviewed briefly in this section. The reader is referred to previous work on the subject for a more detailed treatment.[12,14]

Only uniaxial elongation is discussed in the sequel in order to simplify the discussion. Generalization to any type of strain is obvious, however. Assuming uniaxial elongation along the x axis of a laboratory-fixed Cartesian coordinate system $Oxyz$, the state of macroscopic deformation may be described by the displacement gradient tensor λ as $\lambda = \text{diag}\ (\lambda_x,\lambda_y,\lambda_z)$, where diag denotes the diagonal of the tensor. The off-diagonal terms are zero. λ_x is the extension ratio, i.e., the ratio of the final length of the sample to the initial, undisturbed length, along the direction of stretch, and $\lambda_y = \lambda_z$ are the corresponding ratios along two lateral directions. If the experiment is performed in the swollen state, then $\lambda_x\lambda_y^2 = v_2^{-1}$, where v_2 is the volume fraction of polymer in the swollen network. The effects of isotropic swelling and distortion may be separated by introducing the tensor α, defined as $\alpha = v_2^{1/3}\lambda$, where the x component of α denotes the ratio of the final stretched length to the initial swollen, but undistorted length. If the x component is denoted by α, then $\alpha = \text{diag}\ (\alpha,\alpha^{-1/2},\alpha^{-1/2})$ according to definition.

The corresponding state of deformation at the molecular level requires a more detailed description. Using the molecular model of the network, it is possible to describe microscopic deformations in the mean squared sense.[14] Accordingly, we define two microscopic measures of strain.

The first is the molecular deformation gradient tensor, Λ^2, defined as[14]

$$\Lambda^2 = \begin{bmatrix} \langle x^2\rangle/\langle x^2\rangle_0 & 0 & 0 \\ 0 & \langle y^2\rangle/\langle y^2\rangle_0 & 0 \\ 0 & 0 & \langle z^2\rangle/\langle z^2\rangle_0 \end{bmatrix} \quad (1)$$

where $\langle x^2\rangle$, $\langle y^2\rangle$, and $\langle z^2\rangle$ are the components of the mean-squared end-to-end vector $\langle r^2\rangle$ in the deformed state. The angular brackets denote ensemble averages. The subscript zero refers to the average for the free chain. Equation 1 describes average strain experienced by each chain of the network. It may alternatively be interpreted as the mean strain field that would be observed by a chain if it were embedded in a medium at a state of deformation of Λ^2.

The components of Λ^2 are related to the macroscopic deformation, λ, by the relation[14]

$$\Lambda_t^2 = (1 - 2/\varphi)\lambda_t^2 + (2/\varphi)[1 + B(\lambda_t)] \qquad t = x, y, z \quad (2)$$

where

$$B(\lambda_t) = (\lambda_t - 1)(\lambda_t + 1 - \zeta\lambda_t^2)/[1 + g(\lambda_t)]^2$$
$$g(\lambda_t) = \lambda_t^2[\kappa^{-1} + \zeta(\lambda_t - 1)] \quad (3)$$

Here, φ denotes the junction functionality of the network, κ and ζ are two material parameters: κ denotes the strength of constraints operating on the equilibrium fluctuations in the network, and ζ indicates the effect of inhomogeneities in the network structure.

The second measure of local microscopic strain follows from the consideration of the further transformation of the domains around each junction with macroscopic strain. According to the molecular model,[9] the domains surrounding junctions transform differently in the absence and presence of network connectivity, resulting in a local state of strain, Θ^2, represented as

$$\Theta^2 = \begin{bmatrix} \langle(\Delta S_x)_*^2\rangle/\langle(\Delta S_x)^2\rangle & 0 & 0 \\ 0 & \langle(\Delta S_y)_*^2\rangle/\langle(\Delta S_y)^2\rangle & 0 \\ 0 & 0 & \langle(\Delta S_z)_*^2\rangle/\langle(\Delta S_z)^2\rangle \end{bmatrix} \quad (4)$$

where $(\Delta S_t)_*$ is the t component of the instantaneous fluctuation of a junction from the center of the domain in which it is caught in the network structure. The variables without asterisks refer to the corresponding fluctuations that would obtain in the absence of connectivity.

The ratios appearing in eq 4 are expressed according to theory[14] as

$$\Theta_t^2 = 1 + g(\lambda_t)B(\lambda_t) \quad (5)$$

A segment of a chain in the network is subject to the combined effects of the two deformation fields expressed by eq 2 and 5. Previous work[12] has shown that the segmental orientation function of a deformed network is directly proportional to the deviatoric parts of the combination of the two tensors Λ^2 and Θ^2. Proportionality of Λ^2 reflects the effect of nonaffine transformations of chain dimensions on segmental orientation. Proportionality to Θ^2 reflects the effects of coupling of segments to the surrounding domains.

The tensor Θ^2 may also be regarded as representative of the deformation of the "cage" of local entanglements surrounding a given sequence of bonds. The term cage here alludes to the enveloping domain of a chain. Our treatment does not require a knowledge of the detailed structure of this cage. Prescription of Θ^2 in the manner stated above is sufficient.

Description of Orientation, Mean Mobility, and Anisotropy of Mobility in a Deformed Medium

The kinetics of orientation and mobility has been formulated previously in its most general form.[18] A short summary of the formulation is given in the following paragraphs.

The coordinate system $Oxyz$ in Figure 1a represents the laboratory-fixed system. $\mathbf{n}_0$ is a unit vector affixed to a segment of a chain under consideration. Depending on the spectroscopic technique employed, $\mathbf{n}_0$ will correspond to a C–H bond, a dipole moment, or a transition moment. $\mathbf{n}_0$ defines the orientation of the segment at time t_0, making the spherical polar angles α_0 and β_0 as shown in Figure 1a.

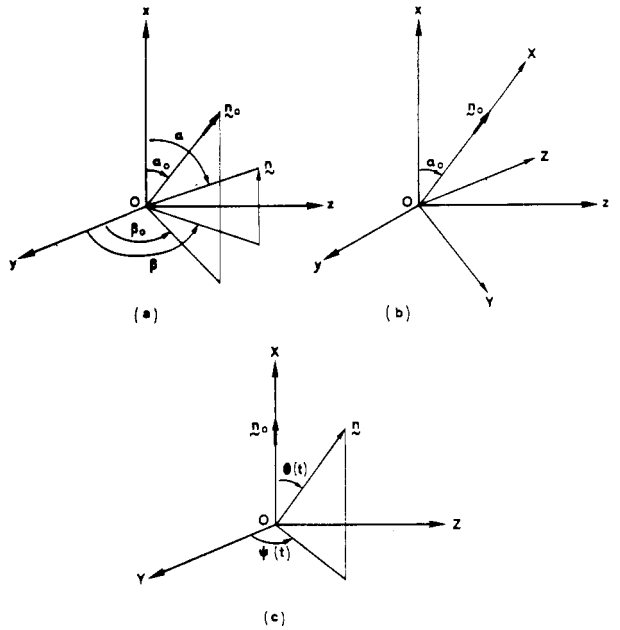

Figure 1. Various coordinate systems for defining the orientation and mobility of a segment whose orientation is represented by the unit vectors $\mathbf{n}_0$ and $\mathbf{n}$ at time t_0 and t, respectively. The $Oxyz$ system is the laboratory-fixed coordinate system, with x denoting the direction of stretch. $OXYZ$ is fixed to the segment and rotates with it. Various spherical angles are defined in the text.

$\mathbf{n}$ denotes the vector $\mathbf{n}_0$ at time $t = t_0 + u$, with spherical polar angles $\alpha(t)$ and $\beta(t)$. The coordinate system $OXYZ$ shown in Figure 1b is affixed to the segment (or to $\mathbf{n}_0$) at time t_0 and is kept fixed with respect to $Oxyz$ for all times. The X axis is along $\mathbf{n}_0$. The Y and Z axes are chosen to make a right-handed Cartesian system, such that the Y axis lies in the plane determined by the x and X axes. At time t, the vector $\mathbf{n}$ makes the spherical polar angles $\theta(t)$ and $\psi(t)$ with the coordinate system $OXYZ$, as shown in Figure 1c. In order to describe the evolution of the orientation of $\mathbf{n}$ in time, the second-order distribution function $P\{\alpha_0,\beta_0;\alpha(t),\beta(t)\}$ is required. The series expansion of P in terms of spherical harmonics may be written as

$$P\{\alpha_0(t_0),\beta_0(t_0);\alpha(t),\beta(t)\} = \sum_{k=0}^{\infty}\sum_{l=0}^{\infty}\sum_{m=-k}^{k}\sum_{n=-l}^{l} f_{kl}^{mn}(t_0,t)\,Y_k^m(\Omega_0)\,\bar{Y}_l^n(\Omega) \quad (6)$$

where $Y_k^m(\Omega_0)$ and $Y_l^n(\Omega)$ are the spherical harmonics with arguments $\Omega_0 = \{\alpha_0,\beta_0\}$ and $\Omega = \{\alpha,\beta\}$, respectively. An overbar denotes the complex conjugate, and

$$f_{kl}^{mn}(t_0,t) = \langle \bar{Y}_k^m(\Omega_0)\,Y_l^n(\Omega)\rangle \quad (7)$$

For the case of uniaxial symmetry considered in this paper, the first six nonzero terms of eq 7 are sufficient to characterize the orientation and mobility of the system. They are f_{00}^{00}, f_{20}^{00}, f_{02}^{00}, f_{22}^{00}, f_{22}^{11}, and f_{22}^{22}. f_{00}^{00} is a constant. The remaining five may be expressed in terms of Ω_0 and Ω as

$$G_{20}^0 \equiv (1/5)^{1/2}(f_{20}^{00}/f_{00}^{00}) = (1/2)\langle 3\cos^2\alpha_0 - 1\rangle$$

$$G_{02}^0 \equiv (1/5)^{1/2}(f_{02}^{00}/f_{00}^{00}) = (1/2)\langle 3\cos^2\alpha - 1\rangle$$

$$G_{22}^0 \equiv (1/5)^{1/2}(f_{22}^{00}/f_{00}^{00}) = (1/4)\langle (3\cos^2\alpha_0 - 1)(3\cos^2\alpha - 1)\rangle$$

$$G_{22}^1 \equiv (3/40)(f_{22}^{11}/f_{00}^{00}) = (9/16)\langle \sin\alpha_0\cos\alpha_0\sin\alpha\cos\alpha\cos(\beta-\beta_0)\rangle$$

$$G_{22}^2 \equiv (3/40)(f_{22}^{22}/f_{00}^{00}) = (9/64)\langle \sin^2\alpha_0\sin^2\alpha\cos[2(\beta-\beta_0)]\rangle \quad (8)$$

In the case of uniaxial symmetry considered in this paper, spectroscopic techniques allow[6,17,18] for the measurement of the functions given by eq 8. The first and second functions of eq 8 are the second Legendre polynomials describing the orientation of the segments at times t_0 and $t = t_0 + u$. For systems at equilibrium, the average orientation does not change with time, and $G_{20}^0 = G_{02}^0$. For transient systems, average orientation depends on t, and hence G_{20}^0 and G_{02}^0 are not equal. In this paper we consider systems in equilibrium only.

The last three functions in eq 8 show correlations between orientation and mobility in different directions in the network. For a clearer physical interpretation, they may be expressed in terms of the coordinate system of Figure 1c by using the transformation

$$Y_l^n(\Omega) = \sum_{\mu=-l}^{l} \bar{D}_{n\mu}^l(\beta_0,\alpha_0)\,Y_l^\mu(\Phi) \quad (9)$$

in eq 7. Here, $D_{m\mu}^l$ are the Wigner matrices and $\Phi = (\theta,\psi)$.

In this way, four new functions M, C, D, and S result instead of the previous three, G_{22}^0, G_{22}^1, and G_{22}^2. M, C, D, and S are expressed in terms of $\theta(t)$ and $\psi(t)$ as

$$M = \langle (3\cos^2\theta(t) - 1)/2\rangle$$

$$C = \langle (3\cos^2\alpha_0 - 1)(3\cos^2\theta(t) - 1)/4\rangle$$

$$D = (3/4)\langle \sin^2\alpha_0\sin^2\theta(t)\cos(2\psi(t))\rangle$$

$$S = 3\langle \sin\alpha_0\cos\alpha_0\sin\theta\cos\theta\cos\psi\rangle \quad (10)$$

M, C, D, and S are related to G_{20}^0, G_{22}^0, G_{22}^1, and G_{22}^2 as

$$M = G_{22}^0 + (16/3)G_{22}^1 + (16/3)G_{22}^2$$

$$4(D - S) = 2G_{20}^0 - 2G_{22}^0 - (16/3)G_{22}^1 + (32/3)G_{22}^2$$

$$3(D - C) = G_{20}^0 - 2G_{22}^0 - (16/3)G_{22}^1 + (32/3)G_{22}^2 \quad (11)$$

The function M is an inverse measure of mean segmental mobility. The term "mean" indicates that mobility of segments is averaged over all directions in the network. M shows the strength of dynamic correlations. It may take values between 0 and 1, where values closer to the former correspond to high mobility and $M = 1$ indicates that the system is frozen between t_0 and $t_0 + u$. C indicates correlations between orientation and mobility. If mobility of segments is uncorrelated with direction, then $C - G_{20}^0 M = 0$. If axial directions have higher (smaller) mobility than the lateral ones, $C - G_{20}^0 M$ is negative (positive). D reflects the directivity of mobility, i.e., the distribution of mobility in planes of different directions. If mobility of segments lying in planes that contain the axis of stretch is larger than those in perpendicular direction, D is positive. S reflects the sense of mobility. For a vector M_0 lying in a plane containing the axis of stretch, for example, a negative (positive) contribution to S results if M_0 orients toward (away from) the axis. The last two expressions of eq 11 indicate that C, D, and S are related to each other by the static orientation correlation function G_{20}^0:

$$D + C - S = G_{20}^0 \quad (12)$$

Various mathematical definitions of the measure of mean mobility and anisotropy of mobility may be introduced[18] by using the moments given in eq 10:

1. Two Different Measures of Average Mobility. (a) Mobility in Terms of the Angular Velocity of n. The angular velocity, ω, of a unit vector $\mathbf{n}_0$ affixed to a segment at time t_0 may be written as $\omega = \mathbf{n}_0 \times \mathbf{n}$, where $\mathbf{n}$ is the vector at time $t_0 + u$. Expressing the components of $\mathbf{n}_0$ and $\mathbf{n}$ in the $Oxyz$ coordinate system and taking the

ensemble average of ω^2 lead to the mean-squared components of ω as

$$\langle \omega_x^2 \rangle = (1/9)(2 - 4G_{20}^0 + 2G_{22}^0 - 32G_{22}^2)$$

$$\langle \omega_y^2 \rangle = \langle \omega_z^2 \rangle = (1/9)(2 + 2G_{20}^0 - 4G_{22}^0 - 16G_{22}^1) \quad (13)$$

Average orientational mobility may be taken as the mean-squared magnitude of ω, which follows from eq 13 and 11 as

$$\langle \omega^2 \rangle = (2/3)(1 - M) \quad (14)$$

It should be noted that the static orientation term G_{20}^0 does not appear in the expression of $\langle \omega^2 \rangle$.

(b) Mean Mobility in Terms of Relaxation Times. The function M describes the time dependence of the molecular rotation angle $\theta(u)$, where u is the time of observation of the system, which was initially observed at $t = 0$. If M would result from a combination of molecular processes characterized by relaxation times τ_i, it could be written as[19]

$$M = \sum_i 1/[1 + (u/\tau_i)^s] \quad (15)$$

where s depends on the type of orientational autocorrelation function; $s = 1$ for exponential relaxation.

Assuming that one of the τ_i is dominant, eq 15 may be written simply as

$$M = 1/[1 + (u/\tau)^s] \quad (15')$$

the term $(u/\tau)^s$ in eq (15′) is a measure of the mobility of the segments. Representing this quantity by m, we have from eq (15′)

$$m \equiv (u/\tau)^s = M^{-1} - 1 \quad (16)$$

In the sequel, we adopt m as the measure of mean segmental orientational mobility. If the segments are frozen, $M = 1$ and $m = 0$. If the segments are infinitely mobile, then $M = 0$ and $m = \infty$.

2. Anisotropy of Mobility. The difference in the mobility of segments in the lateral directions and the longitudinal direction reflects the anisotropy of mobility, A, in the uniaxially deformed network. This difference may be expressed in terms of the lateral and longitudinal components of the mean-squared angular velocity, i.e.

$$A = (1/2)(\langle \omega_y^2 \rangle + \langle \omega_z^2 \rangle) - \langle \omega_x^2 \rangle \quad (17)$$

Using eq 13 and 11, we may write eq 17 as

$$A = (1/3)[G_{20}^0 + (3D - C)] \quad (18)$$

A positive value of A indicates that mobility of vectors along the direction of stretch is higher than those along the lateral direction.

The expressions C and D also reflect anisotropies of motion in the network as discussed above.

Relationship of Orientation, Mean Mobility, and Anisotropy of Mobility to Strain

Recent experiments and theory on segmental orientation[12,13] have shown that the first function of eq 8 may be expressed in terms of the deviatoric components of Λ^2 and Θ^2 as

$$G_{20}^0 = (3/2)D[\Lambda_x^2 - \text{tr}\,(\Lambda^2/3) + e(\Theta_x^2 - \text{tr}\,(\Theta^2/3))] \quad (19)$$

tr denotes the trace operator, and D and e are parameters related to the molecular structure of the network and the strength of coupling of segments to the domains of constraint. Predictions of eq 19 were seen to be in excellent agreement with experimental results.

The dependence of the mean orientational mobility, m, on strain may similarly be explained in terms of the components of Λ^2 and Θ^2. Inasmuch as m corresponds to a quantity averaged over all directions at a point, it can only be a function of invariants of Λ^2 and Θ^2. The most general expression for m should contain the three invariants of Λ^2 and Θ^2. m may suitably be expressed as a Taylor series in these invariants. In this study, we adopt the simplest form of such an expression, where only the first invariants are present in linear combination. Hence

$$m = a[1 + b\,\text{tr}\,(\Lambda^2 - \Lambda_0^2) + c\,\text{tr}\,(\Theta^2 - \Theta_0^2)] \quad (20)$$

where a, b, and c are material coefficients, Λ_0^2 and Θ_0^2 denote values of Λ^2 and Θ^2 for the undistorted, but swollen state (i.e., for $\alpha = 1$), and $\lambda_1 = \lambda_2 = \lambda_3 = v_2^{-1/3}$. For the unswollen, undistorted network, $\text{tr}\,\Lambda_0^2 = \text{tr}\,\Theta_0^2 = 3$.

The expression for m given by eq 20 conveniently separates the effects of distortion of the network from those of isotropic swelling. For the undistorted network

$$m = a(T, v_2) \quad (21)$$

where the dependence of a on temperature and volume fraction of polymer is acknowledged respectively by T and v_2 within the parentheses. Dependence of a on T has been shown[20] to follow the WLF form. Measurements show[17,20] also that m is approximately linear in v_2 in the range 0.85–1.

The coefficient b in eq 20 represents the conformational susceptibility of the chains to change their isomeric states upon deformation of the network.

Assuming that the dynamics is specifically affected when the state of a sequence i changes into a given state η, b may be taken proportional to the statistical quantity $\delta_{2;i,\eta}$, defined by the relationship[21]

$$\delta_{2;i,\eta} = (3/2)[(\langle r_{\eta;i}^2 \rangle_0 / \langle r^2 \rangle_0) - 1] \quad (22)$$

where $\langle r_{\eta;i}^2 \rangle_0$ is the average squared end-to-end vector of a chain for which the sequence i is in state η. $\langle r^2 \rangle_0$ is the average in the absence of this condition. The subscript zero indicates averaging is for the free chain. The coefficient $\delta_{2;i,\eta}$, and hence b, is of the order N^{-1}, where N is the number of bonds in the network strand.

The coefficient c in eq 20 represents the conformational susceptibility of the portions of chains to deformation of the constraint domains in which the mobile unit or sequence is embedded. Additionally, c reflects the effects of the change of the strength of constraints operating on the sequence. In this sense, c is representative of two independent phenomena resulting from conformational and steric effects. To the first-order approximation, b and c should be independent of temperature. Inasmuch as b reflects intramolecular statistics of the single chain, it should be independent of v_2. However, the coefficient c represents effects resulting from the steric coupling of segments to their environments and therefore should depend very strongly on v_2. Its value should vanish at dilutions at which mobility of segments in the network is decoupled from the constraining action of entanglements.

The anisotropy of mobility, A, given by eq 18, reflects the differences in mobility along directions of different deformation ratios. It contains a term proportional to segmental orientation functions, G_{20}^0, and another to $3D - C$. For uniaxial elongation, the term proportional to G_{20}^0 indicates that A increases because the population of mobile segments along the direction of stretch increases relative to that in the lateral directions.

This is the effect of static correlations on anisotropy of mobility. Measurements of mobility on polyisoprene networks (to be reported in the following paper[17]) have indicated that the term $3D - C$ may be equated to zero, within experimental accuracy. For this case, A becomes

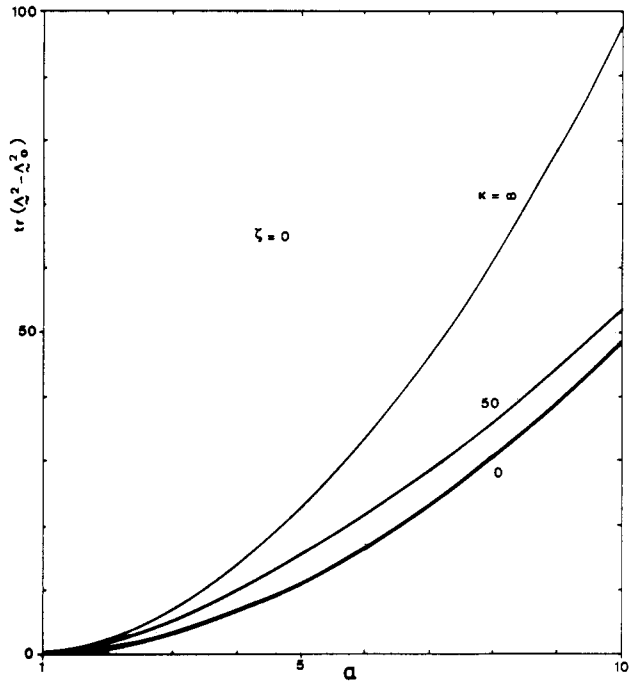

Figure 2. First invariant tr $(\Lambda^2 - \Lambda_0^2)$ of the molecular deformation tensor presented as a function of the elongation ratio α for three values of κ and for $\zeta = 0$. Λ_0^2 is the value of Λ^2 for the undistorted network.

proportional to G_{20}^0 only. Letting $\Lambda_y^2 = \Lambda_z^2$ and $\Theta_y^2 = \Theta_z^2$ for uniaxial extension and using eq 19 in eq 18, we obtain

$$A = (D/3)\{\Lambda_x^2 - \Lambda_y^2 + e(\Theta_x^2 - \Theta_y^2)\} \qquad (23)$$

It should be noted that the term $3D - C$ may not be small, compared to G_{20}^0, for polymeric systems other than polyisoprene, and therefore eq 23 should not be taken as a general expression for anisotropy of mobility.

Numerical Calculations and Discussion

The expressions tr $(\Lambda^2 - \Lambda_0^2)$ and tr $(\Theta^2 - \Theta_0^2)$ that appear in eq 20 describing mean mobility depend strongly on the molecular parameters of the network and on the state of deformation. In Figure 2, values of the scalar quantity tr $(\Lambda^2 - \Lambda_0^2)$ are plotted as a function of extension ratio α for $v_2 = 1$, $\varphi = 4$, and $\zeta = 0$ and for different values of κ. The upper and lower curves correspond to the affine and phantom networks, respectively. The ordinate values indicating the first invariant of the molecular deformation tensor are equal to $\alpha^2 + 2\alpha^{-1} - 3$ for the upper curve. In the phantom network they are half as much. The curve for $\kappa = 50$ lies closer to the one obtained for the phantom network for large extension ratios.

For real networks, κ is in general much less than 50, indicating that the first strain invariant for a real network is closer to that of the phantom one. It should be noted that tr $(\Lambda^2 - \Lambda_0^2)$ increases quadratically with α. This emphasizes that effects of isomerization which are proportional to tr $(\Lambda^2 - \Lambda_0^2)$ are most readily seen at higher deformations.

In Figure 3, values of the invariant tr $(\Theta^2 - \Theta_0^2)$ are plotted as a function of α. For the affine and phantom networks, this invariant is identically zero. For intermediate values of κ, tr $(\Theta - \Theta_0^2)$ differs from zero as seen from the figure. The effect of ζ on tr $(\Theta^2 - \Theta_0^2)$ is very pronounced. In Figure 4, values of tr $(\Theta^2 - \Theta_0^2)$ are presented for different values of ζ. For nonzero values of ζ, the curves exhibit maxima in the vicinity of $\alpha \approx 4$. The curves are calculated for $\kappa = 10$. Calculations for other values of κ also show pronounced maxima.

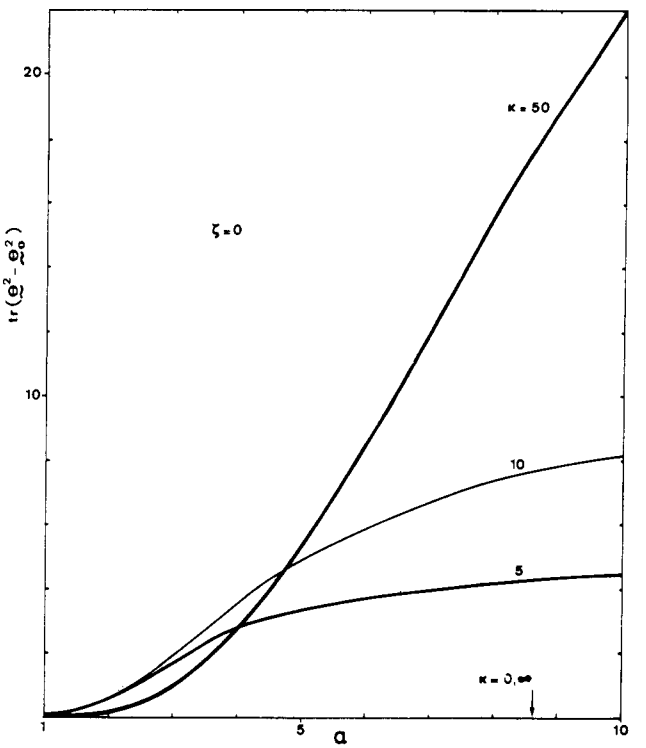

Figure 3. First invariant tr $(\Theta^2 - \Theta_0^2)$ of the deformation tensor of constraint domains presented as a function of the elongation ratio α for three values of κ and for $\zeta = 0$. Θ_0^2 is the value of Θ^2 for the undistorted network.

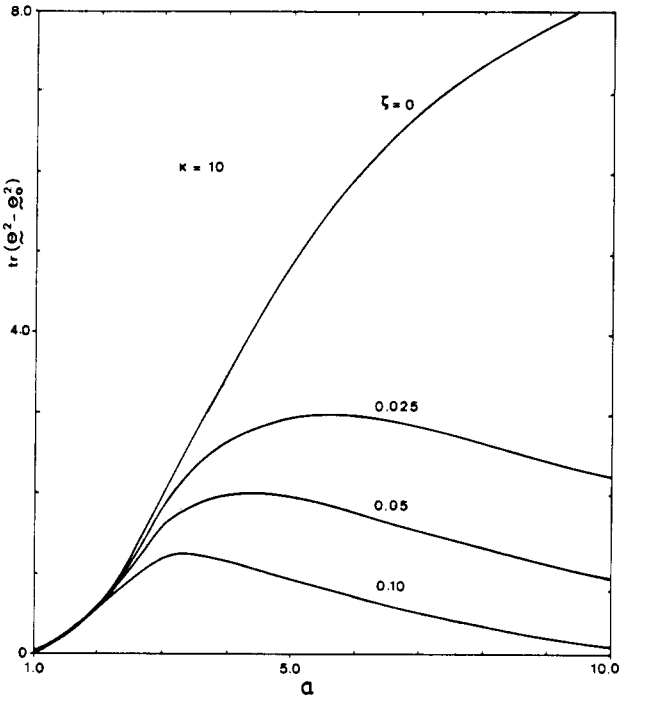

Figure 4. First invariant tr $(\Theta^2 - \Theta_0^2)$ of the deformation tensor of constraint domains presented as a function of α for various values of ζ and for $\kappa = 10$.

The proportionality of mean mobility to the first invariants of the microscopic deformation tensors in the manner given by eq 22 is verified by results of experimental measurements on polyisoprene networks. The pronounced maxima predicted by the theory are observed in all measurements of mobility in dry networks.

Theoretical calculations for anisotropy of mobility A are not given in this paper. As discussed in the above para-

graphs, according to the only available data on networks, A is proportional to the segmental orientation function. Detailed calculations of the segmental orientation function in networks has been given recently.[12]

Acknowledgment. This work was supported by NATO Grant No. 85-0367.

References and Notes

(1) Viovy, J. L.; Monnerie, L.; Brochon, J. C. *Macromolecules* **1983**, *16*, 1845.
(2) Viovy, J. L.; Monnerie, L.; Merola, F. *Macromolecules* **1985**, *18*, 1130.
(3) Viovy, J. L.; Monnerie, L. *Polymer* **1986**, *27*, 181.
(4) Viovy, J. L. Thèse Doctorat ès-Sciences, Paris, 1983.
(5) Viovy, J. L.; Frank, C. W.; Monnerie, L. *Macromolecules* **1985**, *18*, 2607.
(6) Monnerie, L. *Static and Dynamic Properties of the Polymeric Solid State*; Pethrick, R. A., Richards, R. W., Eds.; D. Reidel: Dordrecht, 1982; p 383.
(7) Jasse, B.; Koenig, J. L. *J. Polym. Sci., Polym. Phys. Ed.* **1979**, *17*, 799.
(8) Amram, B.; Bokobza, L.; Queslel, J. P.; Monnerie, L. *Polymer* **1986**, *27*, 877.
(9) Flory, P. J. *J. Chem. Phys.* **1977**, *66*, 5720.
(10) Valeur, B.; Jarry, J. P.; Gény, F.; Monnerie, L. *J. Polym. Sci., Polym. Phys. Ed.* **1975**, *13*, 667, 675.
(11) Helfand, E. H. *J. Chem. Phys.* **1971**, *54*, 4651.
(12) Erman, B.; Monnerie, L. *Macromolecules* **1985**, *18*, 1985.
(13) Queslel, J. P.; Erman, B.; Monnerie, L. *Macromolecules* **1985**, *18*, 1991.
(14) Erman, B.; Flory, P. J. *Macromolecules* **1983**, *16*, 1601.
(15) Erman, B.; Flory, P. J. *Macromolecules* **1983**, *16*, 1607.
(16) Erman, B. *B. Polym. J.* **1985**, *17*, 140.
(17) Jarry, J. P.; Erman, B.; Monnerie, L. *Macromolecules*, following paper in this issue.
(18) Jarry, J. P.; Monnerie, L. *J. Polym. Sci., Polym. Phys. Ed.* **1978**, *16*, 443.
(19) Valeur, B.; Jarry, J. P.; Gény, F.; Monnerie, L. *J. Polym. Sci., Polym. Phys. Ed.* **1975**, *13*, 675.
(20) Jarry, J. P.; Monnerie, L. *Macromolecules* **1979**, *12*, 927.
(21) Abe, Y.; Flory, P. J. *J. Chem. Phys.* **1970**, *52*, 2814.

Segmental Mobility in Deformed Amorphous Polymeric Networks. 2. Experimental Study of Polyisoprene Using the Fluorescence Polarization Technique

J. P. Jarry,† B. Erman,‡ and L. Monnerie*

Laboratoire de Physicochimie Structurale et Macromoléculaire, associé au C.N.R.S., E.S.P.C.I., 10 rue Vauquelin, 75231 Paris Cedex 05, France. *Received April 30, 1986*

ABSTRACT: Results of measurements of segmental mobility by the fluorescence polarization technique are reported for 1,4-*cis*-polyisoprene networks under uniaxial tension at various temperatures and swelling ratios. Experimental data for the mean orientational mobility and anisotropy of mobility resulting from deformation are compared with predictions of the general theory given in the preceding paper.

Introduction

The steady-state dynamics of chains in a deformed network are affected by swelling, temperature, and the state of macroscopic strain. Changes in the dynamics upon deformation depend also on the constitution of the network, determined by factors such as configurational properties of chains and density of cross-linking. Macroscopic distortion of the network, as in the uniaxial stretching experiment, for example, changes the dimensions of chains and of the surrounding domains of local entanglements. The resulting change in configurations of chains and in the strength of local constraints modifies the dynamics to an experimentally measurable extent. In the present paper, results of fluorescence polarization measurements of segmental mobility on deformed polyisoprene networks at equilibrium are reported and compared with theoretical predictions of the preceding paper[1] (called I hereafter).

The fluorescence polarization technique is a convenient method of measuring the orientation and mobility of fluorescent labels attached to specific locations on a small number of chains of the network. The basic principle of the technique rests on the measurement of orientations of labels at two different times, from which the segmental orientation, mean segmental mobility, and dependence of mobility of segments on direction of stretch may be deduced.[2,3]

Fluorescence Polarization Technique

Fluorescence polarization has been used either to study mobility in isotropic systems or to measure the molecular orientation in frozen systems. The theory of this technique has been extended to the case of a uniaxial distribution of molecules[3] and hereafter we briefly review the main conclusions.

The absorption (or emission) properties of a fluorescent molecule can be described through the absorption (or emission) transition moment, $\mathbf{M}_a$ (or $\mathbf{M}_e$). Another characteristic is the mean lifetime, τ, of the excited state of the fluorescent molecule, commonly called the fluorescent lifetime. The most frequent values of τ range from 10^{-9} to 10^{-7} s.

Let us first assume that the transition moments $\mathbf{M}_a$ and $\mathbf{M}_e$ coincide with a molecular axis $\mathbf{M}$ of the fluorophore and that the polarization of the exciting radiation and fluorescence is not affected by the birefringence of the anisotropic sample. The effects arising from delocalization of the transition moments and from birefringence will be dealt with subsequently.

The direction of the unit vector $\mathbf{M}$ is specified by the spherical polar angles $\Omega = (\alpha,\beta)$ with respect to a reference frame $O(x,y,z)$ fixed to the sample, as shown in Figure 1. $N(\Omega_0,t_0)$ is the angular distribution function of $\mathbf{M}$ at time t_0 ($\mathbf{M}_0$ in Figure 1). $P(\Omega,t;\Omega_0,t_0)$ is the conditional probability density of finding at position Ω at time t a vector $\mathbf{M}$

† Permanent address: Rhône-Poulenc Films, Usine St-Maurice de Beynost, 01700 Miribel, France.
‡ Permanent address: School of Engineering, Bogazici University, Bebek, Istanbul, Turkey.

0024-9297/86/2219-2750$01.50/0